Compression mechanism and pressure-induced amorphization of γ-ZrW_2O_8

C. A. Figueirêdo,[1,2] J. Catafesta,[1,2] J. E. Zorzi,[1,2] L. Salvador,[2] I. J. R. Baumvol,[1,2] M. R. Gallas,[2] J. A. H. da Jornada,[2,3] and C. A. Perottoni[1,2,*]

[1]*Universidade de Caxias do Sul, 95070-560 Caxias do Sul, Rio Grande do Sul, Brazil*

[2]*Instituto de Física, Universidade Federal do Rio Grande do Sul, 91501-970 Porto Alegre, Rio Grande do Sul, Brazil*

[3]*Inmetro, Avenida Nossa Senhora das Graças, 50 Xerém, 25250-020 Duque de Caxias, Rio de Janeiro, Brazil*

(Received 10 July 2007; revised manuscript received 24 August 2007; published 1 November 2007)

The structure of γ-ZrW_2O_8 has been optimized at zero pressure and also at $V/V_0=0.97$ by means of density functional theory calculations using the B3LYP functional. As previously found for α-ZrW_2O_8, tungsten polyhedra are stiffer than zirconium octahedra in γ-ZrW_2O_8. However, contrary to what has been found for α-ZrW_2O_8, all first coordination polyhedra in the γ phase are less compressible than the unit cell. Volume reduction in γ-ZrW_2O_8 is, thus, mainly accomplished by polyhedral tilting. Upon pressure increase, the distance between the terminal oxygen and W atoms from the nearest polyhedra decreases by as much as 3.66% (for the pair O101-W6). Accordingly, a further reduction in the zirconium tungstate molar volume with the high-pressure transition to the amorphous phase should bring several oxygen atoms within the threshold of bond formation to W. O 1*s* photoelectron spectra provide further experimental evidence on the formation of additional W-O bonds in amorphous zirconium tungstate. These new W-O bonds should enable the metastable retention of the amorphous phase upon pressure release.

DOI: 10.1103/PhysRevB.76.184201 PACS number(s): 61.50.Ks, 91.60.Ed, 61.43.Er

I. INTRODUCTION

Zirconium tungstate, ZrW_2O_8, is probably the most widely known representative of a class of compounds that exhibit isotropic negative thermal expansion (NTE).[1,2] Despite NTE in zirconium tungstate being already known for decades, there has been a renewed interest in recent years since it was found that this compound exhibits this anomalous behavior over a wide range of temperatures.[3]

At room conditions, zirconium tungstate (α-ZrW_2O_8) is a cubic compound, of space group $P2_13$, with a linear thermal expansion coefficient of -8.8×10^{-6} K^{-1}.[3,4] It is actually a metastable compound with respect to the parent binary oxides at temperatures below 1380 K, and undergoes a phase transition at pressures above 0.2 GPa to γ-ZrW_2O_8, orthorhombic and of space group $P2_12_12_1$.[4–8] The γ phase also exhibits NTE, but the thermal expansion coefficient is one order of magnitude smaller than that of α-ZrW_2O_8.[4] In previous works,[9,10] we have shown that γ-ZrW_2O_8 undergoes an irreversible pressure-induced amorphization (PIA) above about 1.5 GPa. The threshold for PIA can actually be very dependent on the deviatoric stress on the sample. Indeed, we have found that ZrW_2O_8 amorphizes even under heavy grinding in a mortar.[9] Amorphous zirconium tungstate (a-ZrW_2O_8), in turn, recrystallizes into α-ZrW_2O_8 when heated above 900 K at ambient pressure.[9–12]

The NTE of α-ZrW_2O_8 has been attributed to low-energy, transversal vibrational modes [also known as rigid unit modes (RUMs)], involving tilting of nearly rigid polyhedra, whose increase in amplitude leads to contraction on heating.[13,14] Evidences for this low-energy lattice dynamics have been found, among others, in inelastic neutron scattering experiments and low-temperature specific heat measurements.[15,16] More recently, there has been some controversy in the literature regarding details of the microscopic mechanism behind NTE in α-ZrW_2O_8.[17–19] This issue was the subject of a recent paper on the *ab initio* calculation of the structure and elastic properties of α-ZrW_2O_8.[20]

Many other compounds exhibit the same trend between NTE and PIA (see, for instance, Refs. 21 and 22, and references therein). NTE materials, in general, have flexible, open framework structures that may be geometrically or kinetically frustrated in assuming a denser crystalline structure at high pressures and low temperatures.[23,24] Also, owing to their open structures, NTE materials tend to have a molar volume greater than that of the parent oxides from which they are prepared. Hence, volume reduction upon pressure increase becomes a drive force toward decomposition.[25]

Three main mechanisms for PIA of zirconium tungstate have been proposed in the literature. According to the first mechanism, at the early stages of amorphization, some RUMs [or quasi-RUMs (QRUMs)] could provide an energetically favorable route to reduce the framework volume. In some of these RUMs (or QRUMs), the first coordination polyhedral units should run across a point of minimal bent and greater local volume. As the pressure increases, the energy barrier to cross that point of minimal bent becomes greater. The amorphization of zirconium tungstate should, thus, result from the softening of an entire branch of low-energy modes, which freezes the framework structure into a disordered state.[26] Owing to the irreversible character of the transition and the high temperature of recrystallization, some coordination change is expected in amorphous ZrW_2O_8, as new bonds should be formed in order to retain the amorphous phase upon pressure release.[9–12]

PIA of ZrW_2O_8 could also result from a hindered decomposition into ZrO_2 and WO_3.[25] The basis for the hindered decomposition mechanism rests on the fact that the sum of the molar volume of the constituent oxides is smaller than the molar volume of the complex oxide. Accordingly, pressure could drive decomposition in order to reduce volume. Sometimes the decomposition can be kinetically hindered at high pressure and one obtains an amorphous phase. How-

ever, the fact that the simple constituent oxides have the sum of their molar volumes smaller than that of the complex oxide prepared from them is quite common, and it is not restricted to compounds that undergo PIA. Furthermore, one could argue that this mechanism does not account for the observed recrystallization of *a*-ZrW_2O_8 into α-ZrW_2O_8 prior to decomposition.[9–12] Furthermore, recent results from x-ray absorption spectroscopy on amorphous zirconium tungstate are quite different from what would be expected for a hindered decomposition into WO_3 and ZrO_2.[21]

Finally, a α-U_3O_8-type polymorph of ZrW_2O_8 has been obtained at simultaneously high pressure and high temperature.[24] In the α-U_3O_8-type phase of ZrW_2O_8, Zr and W are statistically disordered at the same $3f$ site of space group $P\bar{6}2m$. PIA of ZrW_2O_8 at room temperature could, thus, result from a kinetically impeded transition to this high-pressure, high-temperature crystalline phase.

The refinement of the powder diffraction pattern of a crystal structure such as γ-ZrW_2O_8, with almost 100 internal degrees of freedom, is a formidable task, even at ambient pressure.[7] The lack of a more detailed knowledge of the γ-ZrW_2O_8 crystal structure just prior to amorphization makes it difficult to propose a model for PIA of zirconium tungstate and, thus, critically assess the link between NTE and PIA on topologically soft framework structures. Accordingly, in this paper, we will focus on the effect of pressure on the crystal structure of γ-ZrW_2O_8 based on density functional theory (DFT) calculations. This paper will proceed as follows: In the next section, we will give details of the computational procedure employed to study the effect of pressure on the internal degrees of freedom of the γ-ZrW_2O_8 crystal structure. Next, the high-pressure apparatus used to prepare amorphous zirconium tungstate will be described, along with some details of the x-ray photoelectron spectroscopy (XPS) analysis performed with those samples. Finally, it will be shown how *ab initio* calculations and XPS results both give strong support to W-O bond formation (with the consequent increase of tungsten coordination) in amorphous zirconium tungstate and how this can be related to pressure-induced amorphization in this compound and the metastable retention of the amorphous phase upon pressure release.

II. COMPUTATIONAL DETAILS

All the calculations were performed in the athermal limit with the CRYSTAL03 computer code.[27] The crystalline orbitals were each expressed as a sum of atomic-centered Gaussian functions over all equivalent sites in the periodic system. Total energies were evaluated according to the density functional theory with Becke's gradient-corrected hybrid exchange-correlation density functional (B3LYP).[28] All-electron basis sets were employed for both oxygen[29] and zirconium.[30] For tungsten, we used the Stuttgard-Dresden energy-adjusted 14-valence electron *quasirelativistic* pseudopotential in combination with the corresponding valence basis sets.[31] In the calculations, valence electron f functions and f terms in the pseudopotential had to be omitted for tungsten. The optimized Zr and O all-electron basis sets and W valence electron basis sets were published elsewhere.[20] The tolerances employed in the evaluation of the infinite Coulomb and exchange series were 10^{-6} for the exchange and Coulomb overlap, Coulomb penetration, and the first exchange pseudo-overlap, and 10^{-12} for the second exchange pseudo-overlap tolerance.[27] The Fock matrix has been diagonalized at 64 k points within the irreducible Brillouin zone, corresponding to a shrinkage factor of 6 in the Monkhorst net.[32] The number of k points in the Gilat net was set to 343, corresponding to a shrinkage factor of 12.[33] To improve convergence, a level shifting of 0.5 a.u. was employed and the Fock matrix was updated with a mixing of 30% with the previous Fock matrix at each iteration of the self-consistent-field procedure. To reduce the influence of numerical noise, all the calculations were performed keeping the same set of indexed bielectronic integrals selected from a reference geometry. The tolerance for energy convergence was set to 10^{-6} a.u. Analytical energy derivatives with respect to lattice parameters are not implemented in CRYSTAL03. Accordingly, the γ-ZrW_2O_8 crystal structure at zero pressure was optimized using a three-step procedure. Firstly, the three independent lattice parameters were sequentially optimized, taking as starting point the lattice parameters extrapolated to 0 K as given by Evans *et al.*[8] and keeping the atomic positions fixed at their experimental values.[7] Atomic positions were, thus, optimized at the preoptimized lattice parameters using a modified conjugate gradient algorithm.[34] Convergence was achieved when the maximum gradient and atomic displacement became less than 0.000 45 and 0.0018 a.u., respectively, and root-mean-square gradient and atomic displacement became less than 0.0003 and 0.0012 a.u., respectively. After that, the lattice parameters were reoptimized while keeping the atomic positions fixed at their previously optimized values. Due to the high computational cost, this three-step procedure was performed just one time. The γ-ZrW_2O_8 crystal structure was also optimized at $V/V_0=0.97$. In this case, the lattice parameters were optimized subject to the constraint that the unit cell volume $V=abc$ is fixed. In the sequence, the atomic positions were optimized following the same procedure as before.

III. EXPERIMENT

The sample of α-ZrW_2O_8 used in this work was provided by Wah Chang Co. (Albany, OR). *a*-ZrW_2O_8 was prepared by pressing a pellet of α-ZrW_2O_8 to 7.7 GPa at room temperature in a toroidal high-pressure chamber.[9,35–37] The pressure cell consisted of a graphite container (height of 9.2 mm, diameter of 7.0 mm, and wall thickness of 1.5 mm), two small disks of fired pyrophyllite, and two hBN disks (diameter of 4.0 mm). A capsule of hBN (3.0 mm internal diameter) is placed between these disks, with the sample inside it. In this experimental setup, hBN acts as a nearly isostatic pressure-transmitting medium. The pressure was determined with the aid of a Bi gauge and is considered accurate to ±0.5 GPa.[35–37] The amorphous state of the sample recovered to ambient pressure was checked by x-ray powder diffraction using a Siemens D500 diffractometer.

Chemical bonding was accessed by XPS at a takeoff angle of 45°. The binding energies are referred to the adventitious

carbon C 1*s* line set at 284.8 eV. For curve fitting, a mixture of Gaussian and Lorentzian line shapes (in the proportion of 80/20, respectively) was used for each photoelectron component, according to usual practice, after Shirley background subtraction. A Mg $K\alpha$ (1253.6 eV) x-ray source was used, and the photoelectron energy was analyzed with a typical 0.9 eV resolution.

IV. RESULTS AND DISCUSSION

The crystal structure of γ-ZrW_2O_8 was first optimized at ambient pressure with respect to the three lattice parameters and the atomic positions. All the symmetrically independent atoms in this structure are in general positions, which lead to a total of 99 internal degrees of freedom. Accordingly, at ambient pressure, the optimization of the γ-ZrW_2O_8 structure is accomplished by finding the minimum of the total energy as a function of 102 parameters. This is a huge calculation even for nowadays standards. The resulting crystal structure at ambient pressure is depicted schematically in Fig. 1. In this picture, only oxygen atoms closer than 2.4 Å are represented as bonded to tungsten atoms.

The γ-ZrW_2O_8 crystal structure was also optimized for $V/V_0=0.97$. In this case, the lattice parameters were optimized subject to the constraint that the unit cell volume $V=abc$ is kept constant. The equilibrium lattice parameters were, thus, found by calculating the energies in a 5×5 grid of different b and c (and, correspondingly, a) lattice parameters, always subject to the constraint of constant unit cell volume. A cubic spline interpolating surface was fitted to the calculated energies as a function of b and c. The equilibrium lattice parameters were, thus, obtained by locating the minimum of the interpolating surface (see Fig. 2). In the sequence, the atomic positions were optimized using a modified conjugate gradient algorithm.[34] Although this cannot be considered a thorough optimization, which could be only pursued with a simpler basis set given the available hardware resources, we choose to keep in this work the same basis as used in previous calculations with α-ZrW_2O_8, which rendered excellent results (in particular, for the elasticity tensor).[20]

The lattice parameters calculated for γ-ZrW_2O_8 at ambient pressure and for $V/V_0=0.97$ are given in Table I. Compared to the experimental results of Evans *et al.* extrapolated to 0 K, the DFT results are greater by 1.9%, 2.0%, and 2.5% for the lattice parameters a, b, and c, respectively.[8] This slight overestimation is expected according to the general trend observed with periodic DFT calculations.[38] The lattice parameters a, b, and c diminish with pressure by 0.93%, 0.92%, and 1.11%, respectively, for a 3% reduction of the unit cell volume. The γ-ZrW_2O_8 structure is, thus, about 20% more compressible along the c axis. There is good agreement between the atomic positions calculated at 0 GPa in the athermal limit and the experimental results obtained at ambient pressure and room temperature from Rietveld analysis of neutron powder diffraction patterns.[7,8,39] In going from 0 GPa to $V/V_0=0.97$, the O(102) exhibits greater atomic displacement by moving about 0.09 Å (mainly along the b axis) toward the nearest W1 polyhedron.

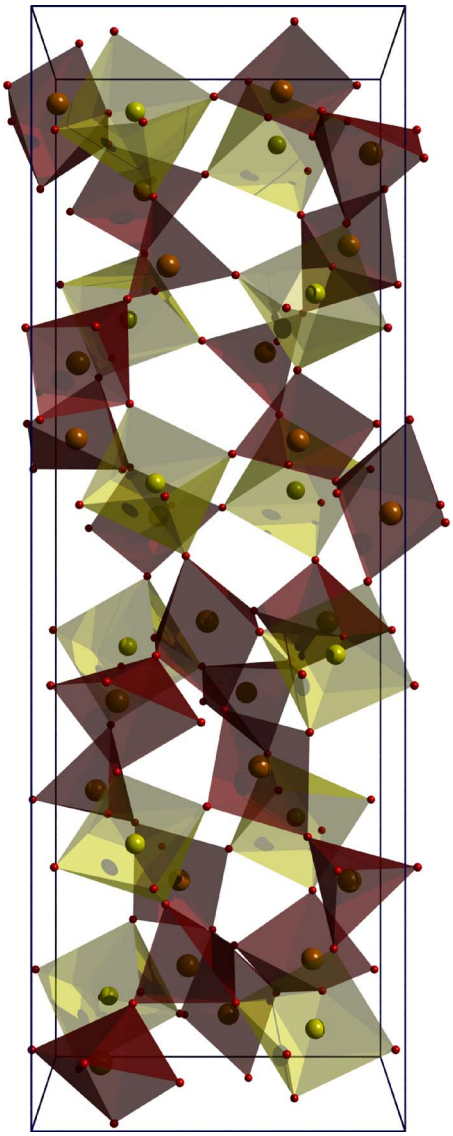

FIG. 1. (Color online) The orthorhombic unit cell of γ-ZrW_2O_8 viewed along the $\bar{1}00$ direction, as optimized at 0 GPa. The yellow (dark red) units represent polyhedra around zirconium and tungsten, respectively.

In the orthorhombic phase, the neighborhood of each tungsten is significantly different.[7] The coordination number, which is 4 for every tungsten in α-ZrW_2O_8, assumes different values from 4 to 4+2 in γ-ZrW_2O_8. Table II shows cation coordination number and the polyhedral volumes for γ-ZrW_2O_8 at $V/V_0=1.0$ and $V/V_0=0.97$. Polyhedral volume was calculated from the optimized atomic positions using IVTON.[40] In these calculations, oxygen atoms with a distance of less than 2.4 Å from tungsten were considered bonded. From bond order calculations, at this distance, an oxygen atom is responsible for more than 4% of the bonding around tungsten [as is the case for the W(4)-O(104) bond at ambient pressure].

Polyhedral tilting has been suggested as the predominant compressibility mechanism in γ-ZrW_2O_8.[7] In fact, according to the data in Table II, the volume reduction of the polyhe-

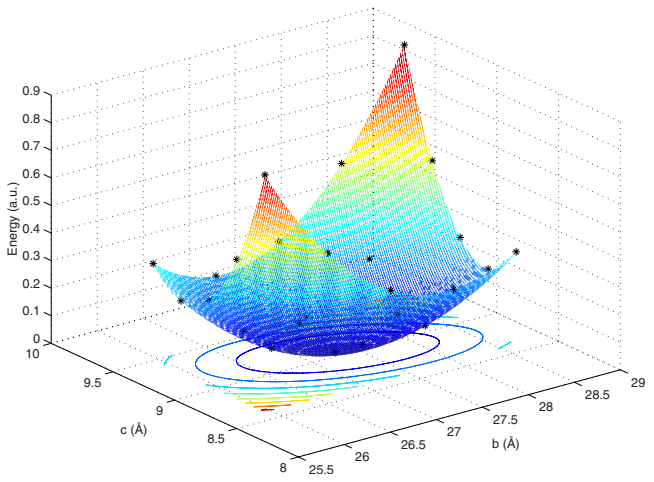

FIG. 2. (Color online) Cubic spline interpolation surface and energies per unit cell (in a.u.) calculated for a grid of 5×5 γ-ZrW_2O_8 b and c lattice parameters subject to the constraint $V/V_0=0.97$.

dral units taken as a whole (1.614 $Å^3$) represents only about 2.4% of the overall volume change of the unit cell. Indeed, the relative volume reduction for the metal-oxygen polyhedra is always lesser than that of the unit cell. This is contrary to what was previously reported for α-ZrW_2O_8, where the zirconium octahedra have been shown to be more compressible than the unit cell.[20] The tungsten polyhedra in γ-ZrW_2O_8 are all less compressible than the octahedra around Zr, as previously found for α-ZrW_2O_8.[20]

Table III shows some interatomic distances in γ-ZrW_2O_8 and their variation when the unit cell volume is reduced by 3%. The distances between the terminal oxygens and W atoms, in general, are greater in α-ZrW_2O_8 (for which the distance W1-O3 is about 2.29 Å at zero pressure, as calculated at the same level of theory[20]) compared to γ-ZrW_2O_8. This is expected owing to the greater molar volume of the former. Indeed, according to our results, γ-ZrW_2O_8 should be 5.3% denser than α-ZrW_2O_8 at zero pressure, in excellent agreement with experimental results.[4,7,41] In fact, taking the experimental lattice parameters for α-ZrW_2O_8 and γ-ZrW_2O_8 near 0 K, the gamma phase should be 5.7% denser than the alpha phase at this temperature.[8,42] With the exception of W(5) and W(6) polyhedra, the mean Zr-O distances are more affected by pressure increase, contributing to the greater compressibility of the Zr octahedra. All tungsten

TABLE I. Comparison between γ-ZrW_2O_8 lattice parameters calculated at the B3LYP density functional theory level and those of Evans *et al.* (Ref. 8) extrapolated to 0 K.

Reference	a (Å)	b (Å)	c (Å)
Evans *et al.*[a]	9.0782	27.045	8.9210
This work ($V/V_0=1.0$)	9.2468	27.586	9.1447
This work ($V/V_0=0.97$)	9.1607	27.314	9.0428

[a]Reference 8.

TABLE II. Cation coordination number and polyhedral volume (in $Å^3$) for γ-ZrW_2O_8 at ambient pressure and $V/V_0=0.97$.

Atom	Coordination	$V/V_0=1.0$	$V/V_0=0.97$	Variation (%)
Zr(1)	6	12.295	11.970	−2.64
Zr(2)	6	12.310	11.982	−2.66
Zr(3)	6	12.312	11.973	−2.75
W(1)	4+1	5.671	5.589	−1.45
W(2)	4+1	5.640	5.567	−1.29
W(3)	4	3.031	3.000	−1.02
W(4)	5	5.801	5.707	−1.62
W(5)	4+2	9.927	9.694	−2.35
W(6)	4+1	5.729	5.620	−1.90

polyhedra become more symmetrical upon pressure increase, as revealed by the reduction of the W-O bond distance standard deviation. Furthermore, it is noteworthy to mention that the distances between terminal oxygen atoms [especially O(101), O(105), and O(103)] and the tungsten atoms of the nearest polyhedra are those that change most. Accordingly, it is reasonable to suppose that a further reduction in the zirconium tungstate molar volume with the transition to the amorphous phase, at high pressure, should bring several oxygen within the threashold of bond formation to W. These new W-O bonds should enable the metastable retention of the amorphous phase upon pressure release.

To further explore this hypothesis, x-ray photoelectron spectroscopy of both α-ZrW_2O_8 and amorphous zirconium tungstate was carried out in order to obtain some experimental evidence about the formation of new W-O bonds in the amorphous phase. Figure 3 shows the O 1s photoelectron spectra of amorphous and α-ZrW_2O_8. While the former shows only a single peak centered at 532.30±0.05 eV, the latter exhibits a wider O 1s signal, which can be deconvoluted into at least two components centered at 532.5±0.2 and 531.3±0.2 eV. These two components can be assigned to bridging (BO) and nonbridging oxygen (NBO), respectively.[43–45] The splitting of the O 1s signal in α-ZrW_2O_8 makes its width [full width at half maximum (FWHM)=2.9±0.1 eV] significantly greater than that in the amorphous phase (FWHM=2.1±0.1 eV). The O 1s XPS peak measured for the amorphous phase is symmetrical, and its maximum coincides (within the experimental uncertainties) with the peak maximum for the BO component in α-ZrW_2O_8. This constitutes strong experimental evidence that the terminal oxygen atoms once present in α-ZrW_2O_8 and γ-ZrW_2O_8 are fully bonded to the neighboring W atoms in amorphous zirconium tungstate. This conclusion is in full agreement with the *ab initio* calculations described above and also with recent results obtained from reverse Monte Carlo analysis of neutron and x-ray total scattering data from a-ZrW_2O_8.[46] Besides that, the formation of additional W-O bonds in a-ZrW_2O_8 is in agreement with the experimentally observed relaxation of the amorphous phase upon pressure release.[21] In fact, even at moderate temperatures, thermal fluctuations should be energetic enough to break some of the

TABLE III. γ-ZrW_2O_8 interatomic distances calculated at 0 GPa and for $V/V_0=0.97$. The mean metal-oxygen distance and its standard deviation (SD) are given for each first coordination polyhedra.

Atom 1	Atom 2	Distance (Å) $V/V_0=1$	Distance (Å) $V/V_0=0.97$	Variation (%)
Zr(1)	O(13)	2.100	2.091	−0.43
	O(22)	2.113	2.096	−0.82
	O(41)	2.174	2.163	−0.55
	O(51)	2.100	2.057	−2.05
	O(53)	2.047	2.051	0.21
	O(61)	2.126	2.090	−1.69
Mean		2.110	2.091	−0.90
SD		0.041	0.039	−4.88
Zr(2)	O(11)	2.168	2.161	−0.30
	O(21)	2.088	2.050	−1.80
	O(23)	2.102	2.071	−1.50
	O(31)	2.192	2.173	−0.86
	O(52)	1.977	1.971	−0.34
	O(63)	2.137	2.116	−0.99
Mean		2.110	2.090	−0.95
SD		0.076	0.075	−1.31
Zr(3)	O(12)	2.068	2.058	−0.47
	O(32)	2.146	2.128	−0.86
	O(33)	2.199	2.182	−0.77
	O(42)	2.100	2.071	−1.38
	O(43)	2.077	2.061	−0.77
	O(62)	2.078	2.053	−1.21
Mean		2.111	2.092	−0.90
SD		0.051	0.052	1.96
W(1)	O(11)	1.814	1.811	−0.16
	O(12)	1.834	1.821	−0.70
	O(13)	1.838	1.832	−0.35
	O(101)	1.806	1.816	0.54
	O(102)	2.233	2.186	−2.12
Mean		1.905	1.893	−0.63
SD		0.184	0.164	−10.9
W(2)	O(21)	1.845	1.852	0.39
	O(22)	1.853	1.839	−0.75
	O(23)	1.829	1.824	−0.26
	O(102)	1.791	1.794	0.18
	O(105)	2.168	2.106	−2.87
Mean		1.897	1.883	−0.74
SD		0.153	0.126	−17.6
W(3)	O(31)	1.807	1.796	−0.64
	O(32)	1.812	1.813	0.10
	O(33)	1.829	1.817	−0.67
	O(104)	1.786	1.784	−0.10
Mean		1.808	1.802	−0.33
SD		0.018	0.015	−16.7
W(4)	O(41)	1.826	1.821	−0.32
	O(42)	1.850	1.839	−0.60
	O(43)	1.836	1.830	−0.31
	O(103)	1.783	1.788	0.27
	O(104)	2.313	2.268	−1.94
Mean		1.921	1.909	−0.62
SD		0.220	0.201	−8.63
W(5)	O(51)	1.829	1.822	−0.36
	O(52)	1.892	1.880	−0.59
	O(53)	1.857	1.853	−0.24
	O(103)	2.370	2.309	−2.58
	O(105)	1.804	1.814	0.53
	O(106)	2.104	2.068	−1.70
Mean		1.976	1.958	−0.91
SD		0.221	0.196	−11.3
W(6)	O(61)	1.814	1.820	0.35
	O(62)	1.829	1.827	−0.10
	O(63)	1.814	1.800	−0.77
	O(101)	2.282	2.199	−3.66
	O(106)	1.808	1.808	−0.02
Mean		1.909	1.891	−0.94
SD		0.209	0.173	−17.2

weaker W-O bonds formed under pressure, leading to the irreversible length change of a-ZrW_2O_8 upon annealing, even before recrystallization.[12] Taking $T=900$ K as the onset temperature for the recrystallization of a-ZrW_2O_8 into α-ZrW_2O_8 (Ref. 11) (which should be accomplished by extensive W-O bond breaking), it is possible to estimate an upper limit of about $kT\approx 0.08$ eV for the energies associated with the additional W-O bonds bridging the tungsten polyhedra in the amorphous structure.

The picture that emerges from these results can be summarized as follows: At high pressure, the formation of a large number of incommensurate structures due to the softening of an entire vibrational branch leads to the amorphization of γ-ZrW_2O_8, and is accompanied by the continuous accumulation of local defects, represented by the disordered formation of new W-O bonds.[47–49] The volume reduction due to the formation of new W-O bonds should release stress locally, hindering the formation of additional W-O bonds around newly formed ones and precluding the evolution toward a high-pressure crystalline phase. The additional W-O bonds also enable the metastable retention of a-ZrW_2O_8 upon pressure release.

The findings reported here probably are common to other open framework structures that exhibit both NTE and PIA, and also have terminal oxygen atoms. In fact, in the absence of a soft mode crystal-to-crystal phase transition (or in the case such transition is kinetically hindered), the softening of a large number of low-energy modes should freeze these

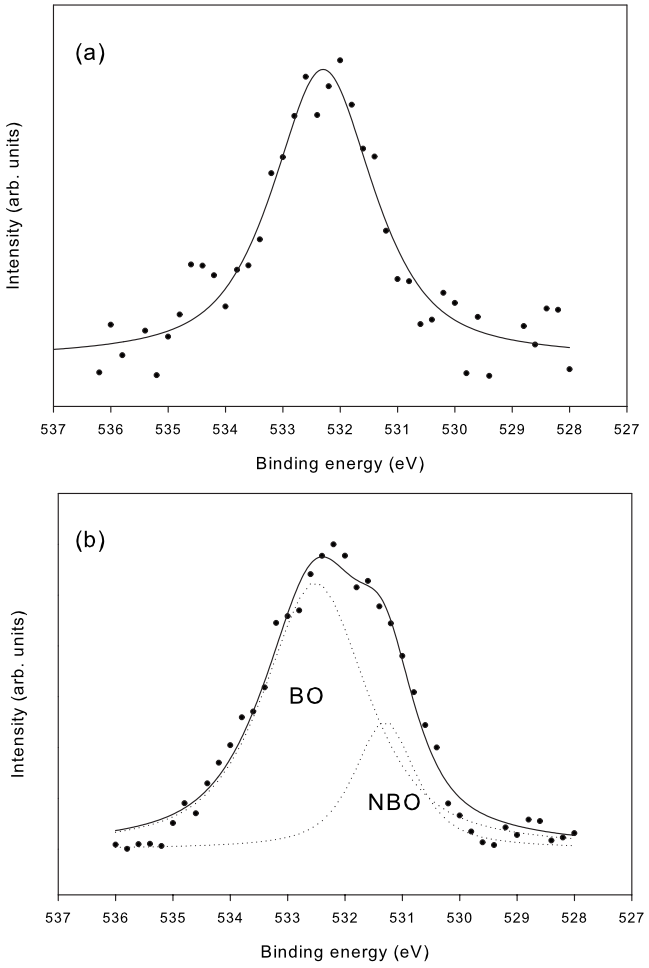

FIG. 3. O 1*s* photoelectron spectrum of (a) amorphous zirconium tungstate and (b) α-ZrW_2O_8. In (b) the bridging and nonbridging O 1*s* peaks are denoted by BO and NBO, respectively.

open framework structures into a disordered state. This x-ray amorphous state should be quenchable to ambient pressure as long as some additional bonds involving terminal oxygen atoms could be formed at high pressure. Calculations are under way to test some observable consequences of this hypothesis.

V. CONCLUSION

The evolution with pressure of the γ-ZrW_2O_8 crystal structure has been studied by means of computer simulations. Also, O 1*s* x-ray photoelectron spectra at ambient pressure were obtained for α-ZrW_2O_8 and amorphous zirconium tungstate. *Ab initio* calculations show that volume reduction of γ-ZrW_2O_8 under pressure is mainly accomplished by polyhedral tilting. The calculations also show that a 3% reduction in the unit cell volume leads to a noticeable decrease in the distance between terminal oxygen atoms and the W atoms of the nearest polyhedra. A further reduction in the molar volume with the transition to the amorphous phase should bring several oxygen within the threshold of bond formation to W. The formation of new W-O bonds in *a*-ZrW_2O_8 is further supported by results from O 1*s* x-ray photoelectron spectroscopy. These new bonds increase tungsten coordination and should be responsible for the metastable retention of the amorphous phase upon pressure release. The progressive breaking of these additional W-O bonds should be at the origin of the relaxation effects previously observed upon annealing of amorphous zirconium tungstate.[12] This feature should, thus, be taken into account in any mechanism proposed to explain PIA of zirconium tungstate.

ACKNOWLEDGMENTS

The authors thank Jim Walker, from Wah Chang Co. (Albany, OR), for the sample of zirconium tungstate used in this work, and André Martinotto, Ricardo Dorneles Vargas (DEIN/UCS), and Günther Gerhardt (DEFQ/UCS), who granted access to the computer clusters where most of the calculations presented in this paper were performed. This work was partially supported by the Brazilian agencies PRONEX/MCT, CNPq, CAPES, and FAPERGS.

*caperott@ucs.br

[1] J. Graham, A. D. Wadsley, J. H. Weymouth, and L. S. Williams, J. Am. Ceram. Soc. **42**, 570 (1959).
[2] C. Martinek and F. A. Hummel, J. Am. Ceram. Soc. **51**, 227 (1968).
[3] T. A. Mary, J. S. O. Evans, T. Vogt, and A. W. Sleight, Science **272**, 90 (1996).
[4] J. S. O. Evans, Z. Hu, J. D. Jorgensen, D. N. Argyriou, S. Short, and A. W. Sleight, Science **275**, 61 (1997).
[5] L. L. Y. Chang, M. G. Scroger, and B. Phillips, J. Am. Ceram. Soc. **50**, 211 (1967).
[6] C. Pantea, A. Migliori, P. B. Littlewood, Y. Zhao, H. Ledbetter, J. C. Lashley, T. Kimura, J. Van Duijn, and G. R. Kowach, Phys. Rev. B **73**, 214118 (2006).
[7] J. D. Jorgensen, Z. Hu, S. Teslic, D. N. Argyriou, S. Short, J. S. O. Evans, and A. W. Sleight, Phys. Rev. B **59**, 215 (1999).
[8] J. S. O. Evans, J. D. Jorgensen, S. Short, W. I. F. David, R. M. Ibberson, and A. W. Sleight, Phys. Rev. B **60**, 14643 (1999).
[9] C. A. Perottoni and J. A. H. da Jornada, Science **280**, 886 (1998).
[10] A. S. Pereira, C. A. Perottoni, and J. A. H. da Jornada, J. Raman Spectrosc. **34**, 578 (2003).
[11] C. A. Perottoni, J. E. Zorzi, and J. A. H. da Jornada, Solid State Commun. **134**, 319 (2005).
[12] J. Catafesta, J. E. Zorzi, C. A. Perottoni, M. R. Gallas, and J. A. H. da Jornada, J. Am. Ceram. Soc. **89**, 2341 (2006).
[13] A. W. Sleight, Annu. Rev. Mater. Sci. **28**, 29 (1998).
[14] A. K. A. Pryde, K. D. Hammonds, M. T. Dove, V. Heine, J. D. Gale, and M. C. Warren, J. Phys.: Condens. Matter **8**, 10973 (1996).
[15] G. Ernst, C. Broholm, G. R. Kowach, and A. P. Ramirez, Nature

(London) **396**, 147 (1998).
[16] A. P. Ramirez and G. R. Kowach, Phys. Rev. Lett. **80**, 4903 (1998).
[17] M. G. Tucker, A. L. Goodwin, M. T. Dove, D. A. Keen, S. A. Wells, and J. S. O. Evans, Phys. Rev. Lett. **95**, 255501 (2005).
[18] D. Cao, F. Bridges, G. R. Kowach, and A. P. Ramirez, Phys. Rev. Lett. **89**, 215902 (2002).
[19] D. Cao, F. Bridges, G. R. Kowach, and A. P. Ramirez, Phys. Rev. B **68**, 014303 (2003).
[20] C. A. Figueirêdo and C. A. Perottoni, Phys. Rev. B **75**, 184110 (2007).
[21] T. Varga, A. P. Wilkinson, A. C. Jupe, C. Lind, W. A. Bassett, and C. S. Zha, Phys. Rev. B **72**, 024117 (2005).
[22] S. K. Sikka, J. Phys.: Condens. Matter **16**, S1033 (2004).
[23] A. P. Ramirez, C. L. Broholm, R. J. Cava, and G. R. Kowach, Physica B **280**, 290 (2000).
[24] A. Grzechnik, W. A. Crichton, K. Syassen, P. Adler, and M. Mezouar, Chem. Mater. **13**, 4255 (2001).
[25] A. K. Arora, V. S. Sastry, P. Ch. Sahu, and T. A. Mary, J. Phys.: Condens. Matter **16**, 1025 (2004).
[26] S. M. Sharma and S. K. Sikka, Prog. Mater. Sci. **40**, 1 (1996).
[27] V. R. Saunders *et al.*, *CRYSTAL2003 User's Manual* (University of Torino, Torino, 2003).
[28] A. D. Becke, J. Chem. Phys. **98**, 5648 (1993).
[29] R. Dovesi, C. Roetti, C. Freyria-Fava, M. Prencipe, and V. R. Saunders, Chem. Phys. **156**, 11 (1991).
[30] R. Dovesi and S. Gennard, http://www.crystal.unito.it/Basis_Sets/zirconium.html
[31] D. Andrae, U. Häußermann, M. Dolg, H. Stoll, and H. Preuß, Theor. Chim. Acta **77**, 123 (1990); see also http://www.theochem.uni-stuttgart.de
[32] H. J. Monkhorst and J. D. Pack, Phys. Rev. B **13**, 5188 (1976).
[33] G. Gilat and J. L. Raubenheimer, Phys. Rev. **144**, 390 (1966).
[34] H. B. Schlegel, J. Comput. Chem. **3**, 214 (1982).
[35] W. F. Sherman and A. A. Stadtmüller, *Experimental Techniques in High Pressure Research* (Wiley, New York, 1987), Chap. 6.
[36] L. G. Khvostantsev, High Temp. - High Press. **16**, 165 (1984).
[37] M. I. Eremets, *High Pressure Experimental Methods* (Oxford University Press, New York, 1996), Chap. 2.
[38] A. Zupan and M. Causà, Int. J. Quantum Chem. **56**, 337 (1995).
[39] See EPAPS Document No. E-PRBMDO-76-047738 for a comparison between atomic positions optimized at $P=0$ and $V/V_0=0.97$, and some experimental results obtained at ambient pressure and room temperature from Rietveld analysis of neutron powder diffraction patterns (Refs. 7 and 8). For more information on EPAPS, see http://www.aip.org/pubservs/epaps.html.
[40] T. Balic Zunic and I. Vickovic, J. Appl. Crystallogr. **29**, 305 (1996).
[41] Z. Hu, J. D. Jorgensen, S. Teslic, S. Short, D. N. Argyriou, J. S. O. Evans, and A. W. Sleight, Physica B **241-243**, 370 (1998).
[42] J. S. O. Evans, W. I. F. David, and A. W. Sleight, Acta Crystallogr., Sect. B: Struct. Sci. **55**, 333 (1999).
[43] A. Hayashi, M. Tatsumisago, and T. Minami, J. Am. Ceram. Soc. **81**, 1305 (1998).
[44] R. Gresch, W. Müller-Warmuth, and H. Dutz, J. Non-Cryst. Solids **34**, 127 (1979).
[45] R. Brücner, H.-U. Chun, H. Goretzki, and M. Sammet, J. Non-Cryst. Solids **42**, 49 (1980).
[46] D. A. Keen, A. L. Goodwin, M. G. Tucker, M. T. Dove, J. S. O. Evans, W. A. Crichton, and M. Brunelli, Phys. Rev. Lett. **98**, 225501 (2007).
[47] A. K. Arora, T. Yagi, N. Miyajima, and T. A. Mary, J. Appl. Phys. **97**, 013508 (2005).
[48] H. J. Fecht, Nature (London) **356**, 133 (1992).
[49] H. Trinkaus, Mater. Sci. Forum **248-249**, 3 (1997).